



Cite this: *Chem. Commun.*, 2024, 60, 10410

Received 18th June 2024,  
Accepted 22nd August 2024

DOI: 10.1039/d4cc02943g

rsc.li/chemcomm

# Twisted diphenoquinones fused with thiophene rings: thiophene analogs of bianthrone†

Yohei Adachi,<sup>a</sup> Yuto Hattori,<sup>a</sup> Tsubasa Mikie,<sup>b</sup> Itaru Osaka<sup>b</sup> and Joji Ohshita<sup>a,c</sup>

The twisted conformer of bistricyclic aromatic enes (BAEs) has a small HOMO–LUMO gap owing to the twisted double bond. In this study, we synthesized diphenoquinones fused with thiophene rings as a new twisted conformer-predominant BAE. They exhibited deep LUMO energy levels and apparent n-type semiconductor properties.

$\pi$ -Conjugated materials are widely used in various applications such as organic electronics and imaging materials thanks to their distinctive characteristics such as photoabsorption in the UV-vis-NIR region and semiconducting properties. In order to induce a bathochromic shift in the photoabsorption, the  $\pi$ – $\pi^*$  energy gap must be decreased. This can be achieved by extending the  $\pi$ -conjugation,<sup>1a–c</sup> utilizing intramolecular donor–acceptor interactions<sup>1a–c</sup> and increasing quinoidal character,<sup>1d</sup> which, unfortunately, results in large molecular structures or requires multistep synthesis. Therefore, new molecular designs that realize long-wavelength absorption in small and simple structures are desired. On the other hand, the twisting of the double bond decreases the overlap between the two p-orbitals, leading to increased reactivity, a biradical character, and a low-energy triplet state.<sup>2</sup> In addition to these characteristics, the twisting of the double bond leads to a decrease in the transition energy by decreasing the energy gap between the  $\pi/\pi^*$  orbitals (Fig. 1a), which is an important consideration in the design of molecules for the development of  $\pi$ -conjugated materials with a small HOMO–LUMO gap. For example, 9,9'-bifluorenylidene, a typical example of bistricyclic aromatic enes (BAEs),<sup>3</sup> is known

to have a twisted conformer to avoid steric hindrance in the fjord region (Fig. 1b). Its central double bond has a dihedral angle of 42°, and its maximum absorption wavelength (458 nm in CH<sub>2</sub>Cl<sub>2</sub>)<sup>4</sup> is much longer than that of dibenzo[*g,p*]chrysene (351 nm in CH<sub>2</sub>Cl<sub>2</sub>),<sup>5</sup> a planar structural isomer of 9,9'-bifluorenylidene. In BAEs, which does not contain fluorenylidene for the tricyclic structures, a conformational isomer called the folded conformer, in which the tricyclic structures are folded and there is no twisting in the double bond, is generally more thermodynamically stable than its twisted counterpart.<sup>3</sup> For example, bianthrone, which is a diphenoquinone fused with benzene rings, shows thermochromism,<sup>6</sup> predominantly exists as a folded conformer, and is light yellowish at room temperature owing to the large HOMO–LUMO gap (Fig. 1b). Whereas various homomeric<sup>7</sup> and heteromeric BAEs<sup>8</sup> have been reported, twisted-conformer-predominant BAEs are limited to those containing a five-membered ring structure such as fluorenylidene,<sup>4,9</sup> and their structures have

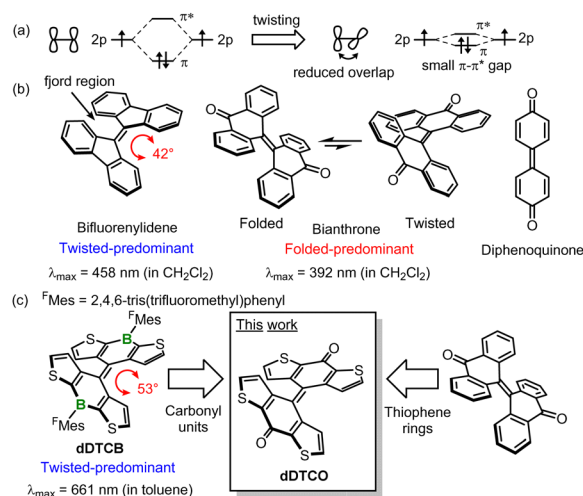


Fig. 1 (a) Schematic diagram of the energy changes in  $\pi/\pi^*$  orbitals due to the twisting of a double bond. Structures of BAEs based on benzene rings (b) and thiophene rings (c).

<sup>a</sup> Smart Innovation Program, Graduate School of Advanced Science and Engineering, Hiroshima University, Higashi-Hiroshima 739-8527, Japan. E-mail: yadachi@hiroshima-u.ac.jp, jo@hiroshima-u.ac.jp

<sup>b</sup> Applied Chemistry Program, Graduate School of Advanced Science and Engineering, Hiroshima University, Higashi-Hiroshima 739-8527, Japan

<sup>c</sup> Division of Materials Model-Based Research, Digital Monozukuri (Manufacturing) Education and Research Center, Hiroshima University, 3-10-32 Kagamiyama, Higashi-Hiroshima, Hiroshima 739-0046, Japan

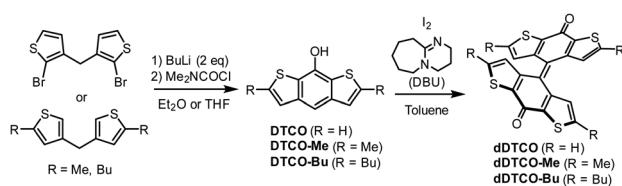
† Electronic supplementary information (ESI) available. CCDC 2363404–2363406. For ESI and crystallographic data in CIF or other electronic format see DOI: <https://doi.org/10.1039/d4cc02943g>



limited diversity. As a new strategy to control the energy of BAE conformers, we have focused on the use of heterocycles such as thiophene. The more compact structure of thiophene than benzene is expected to markedly influence the electronic structures and the steric hindrance in BAEs. Indeed, we previously reported that the twisted conformer of **ddTCB** (Fig. 1c), a BAE comprised of thiophene rings and boron, was thermodynamically stable.<sup>10</sup> However, the synthesis of **ddTCB** was complicated owing to the presence of tricoordinate boron in the structure. In this study, we designed **ddTCO**, a simple structured diphenoquinone fused with thiophene rings, by substituting  $sp^2$  carbonyl units for the  $sp^2$  boron units of **ddTCB**, as a new twisted-predominant BAE (Fig. 1c). All benzene rings in bianthrone were replaced by thiophene rings in **ddTCO**. The first synthesis of **ddTCO** was reported by the Mazaki group,<sup>11</sup> but as far as we know, the detailed synthesis methods and properties of the compound have not been reported.

The synthesis of **ddTCO** was accomplished similarly to that of **ddTCB** (Scheme 1).<sup>10a</sup> The precursor of **ddTCO**, **DTCO**, was more stable in its enol form than its keto form as only the phenol form was observed in the  $^1\text{H}$  NMR spectrum.<sup>12</sup> We found that **DTCO** was unstable in air; it gradually converted into a quinone upon standing in air both in solution and in the solid state (Fig. S1, ESI†). Therefore, **DTCO** was used in the subsequent dimerization reaction immediately after synthesis. **DTCO** quickly dimerized at low temperatures in the presence of iodine and 1,8-diazabicyclo[5.4.0]undec-7-ene (DBU), yielding the desired thiophene-fused diphenoquinone (**ddTCO**) as a dark purple solid. **ddTCO** was stable in air, showing no decomposition even after storage for more than one year in air in the solid state. In contrast to bianthrone that readily undergoes photocyclization,<sup>13</sup> **ddTCO** showed very high photostability (Fig. S2, ESI†). **ddTCO** exhibited poor solubility, being soluble in chloroform but scarcely soluble in toluene or acetone, whereas alkylated derivatives **ddTCO-Me** and **ddTCO-Bu** exhibited better solubility. In particular, **ddTCO-Bu** dissolved completely in toluene. In the  $^1\text{H}$  NMR spectrum of **ddTCO**, only two sharp doublet signals corresponding to the protons on the thiophene rings were observed (Fig. S3, ESI†), suggesting that only one isomer is predominantly present in solution.

Next, single-crystal X-ray diffraction analyses were performed. As expected, all the X-ray structures of the thiophene-fused diphenoquinones showed twisted conformers similar to **ddTCB** (Fig. 2 and Fig. S4, ESI†).<sup>10a</sup> This contrasted with the folded X-ray structure of bianthrone,<sup>7c</sup> suggesting that the substitution of thiophene rings for the benzene rings in bianthrone thermodynamically stabilized the twisted conformer



Scheme 1 Synthesis of **ddTCO** and its alkylated derivatives.

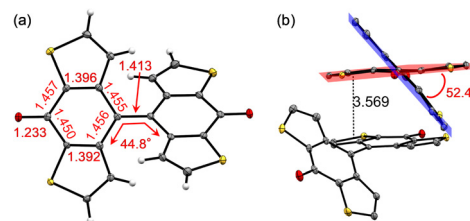


Fig. 2 Monomeric crystal structure with bond lengths in Å (a) and dimeric crystal structure with dihedral angle between the mean planes of the tricyclic structures (b) of **ddTCO** obtained at 100 K. Thermal ellipsoids are at 50% probability level.

relative to the folded conformer. In our previous work, the twist angle of the central double bond was defined by the dihedral angle of the four carbon atoms around the double bond (Fig. 2a).<sup>10a</sup> However, for comparison with other studies, here we focused on the dihedral angle between the mean planes of the tricyclic structures (Fig. 2b). The dihedral angle of **ddTCO** was  $52.4^\circ$ , which was much larger than that of 9,9'-bifluorenylidene ( $42^\circ$ ).<sup>4</sup> Although this dihedral angle was slightly smaller than that of **ddTCB** ( $53.4^\circ$ , Fig. S5, ESI†),<sup>10a</sup> the difference was only  $1.0^\circ$ . The central C=C double bond of **ddTCO** was  $1.41 \text{ \AA}$ , much longer than that of bianthrone ( $1.36 \text{ \AA}$ ),<sup>7c</sup> indicating the decreased double bond character in **ddTCO**. Bond alternation in the diphenoquinone structure of **ddTCO** was smaller than that of bianthrone (Table S1, ESI†), suggesting the highly conjugated structure of **ddTCO** within the diphenoquinone structure. The monomeric X-ray structures of **ddTCO-Me** and **ddTCO-Bu** were similar to that of **ddTCO** (Fig. S4 and S5, ESI†). Interestingly, despite the twisted structure, **ddTCO** exhibited a dense packing structure with a  $\pi$ - $\pi$  distance of  $3.57 \text{ \AA}$  between two molecules (Fig. 2b), indicating the presence of weak  $\pi$ - $\pi$  interactions. In alkylated derivatives **ddTCO-Me** and **ddTCO-Bu**, the intermolecular distances were larger than that of **ddTCO** (Fig. S4, ESI†). The powder X-ray diffraction pattern of **ddTCO** well matched the pattern simulated from the single-crystal X-ray data (Fig. S6, ESI†).

The UV-vis absorption spectra of the thiophene-fused diphenoquinones in  $\text{CH}_2\text{Cl}_2$  are shown in Fig. 3. The strong absorption of **ddTCO** in the long-wavelength region with a maximum at  $608 \text{ nm}$  is a typical characteristic of twisted BAEs (Table 1).<sup>4,9,10a</sup> Generally, the absorption band shifts to the longer wavelength region as the twist angle of the central double bond

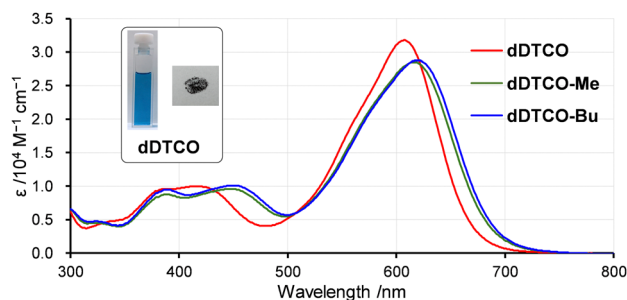


Fig. 3 UV-vis absorption spectra of thiophene-fused diphenoquinones in  $\text{CH}_2\text{Cl}_2$  at the concentration of  $0.01 \text{ mM}$ .



**Table 1** Optical and electrochemical data of thiophene-fused diphenylquinones in CH<sub>2</sub>Cl<sub>2</sub>

Compound	$\lambda_{\text{max}}^a/\text{nm}$	$E_{\text{ox}}^b/\text{V}$	$E_{\text{red}}^c/\text{V}$	HOMO <sup>d</sup> /eV	LUMO <sup>e</sup> /eV
<b>ddTCO</b>	608	1.01	−0.655	−5.81	−4.15
<b>ddTCO-Me</b>	613	0.895	−0.680	−5.70	−4.12
<b>ddTCO-Bu</b>	617	0.902	−0.698	−5.70	−4.10

<sup>a</sup> Absorption maximum. <sup>b</sup> Onset potential of the first oxidation wave in CV (vs. Fc/Fc<sup>+</sup>). <sup>c</sup> Half-wave potential of the first reduction wave in CV (vs. Fc/Fc<sup>+</sup>). <sup>d</sup> HOMO = −4.8 −  $V_{\text{ox}}$ . <sup>e</sup> LUMO = −4.8 −  $V_{\text{red}}$ .

increases. The dihedral angles in the X-ray structures are ordered as follows: 9,9'-bifluorenylidene < **ddTCO** < **ddTCB**,<sup>4,10a</sup> and accordingly, the absorption maxima are red-shifted. In addition, 1,1',4,4'-tetramethyl-9,9'-bifluorenylidene, which has methyl groups in the fjord region of 9,9'-bifluorenylidene to increase the steric hindrance,<sup>4</sup> has a dihedral angle of 56°, larger than that of **ddTCO**. Nonetheless, its absorption maximum in CH<sub>2</sub>Cl<sub>2</sub> is 485 nm, much shorter than that of **ddTCO**. One reason for this is that the aromaticity of thiophene is lower than that of benzene, which effectively extended the conjugation within the molecule for **ddTCO**.<sup>14</sup> The molar absorption coefficient of **ddTCO** at 608 nm was 31 800 M<sup>−1</sup> cm<sup>−1</sup>, which is similar to that of twisted-conformer-dominant **ddTCB** ( $\epsilon$  = 32 200 M<sup>−1</sup> cm<sup>−1</sup> at 655 nm in CH<sub>2</sub>Cl<sub>2</sub>).<sup>10a</sup> The absorption maximum of the folded-predominant BAE of bianthrone is around 392 nm in the UV region,<sup>7c</sup> revealing a significant impact of the aromatic ring substitution on the electronic structures of BAEs. The absorption maxima of **ddTCO-Me** and **ddTCO-Bu** were slightly red-shifted from that of **ddTCO** owing to the inductive effect of the alkyl groups (Fig. 3). Solvent dependence was not observed in the absorption spectra of **ddTCO** (Fig. S7, ESI†). In the solid-state UV-vis absorption spectrum of **ddTCO**, the absorption band shifted to longer wavelengths than in solution, probably due to  $\pi$ - $\pi$  interactions in the solid state (Fig. S8, ESI†).

To investigate the influence of each structure on the energy of the conformers, the twisted and folded conformers of **ddTCO** and bianthrone were optimized in DFT calculations (Fig. 4 and Fig. S9, S10, ESI†). The optimized structures of **ddTCO** and bianthrone were in good agreement with the single-crystal X-ray structures (Fig. 4 and Fig. S9, ESI†).<sup>7c</sup> Whereas the folded conformer was 13.2 kJ mol<sup>−1</sup> more stable than the twisted conformer in bianthrone, in the case of **ddTCO**, the twisted conformer was 34.5 kJ mol<sup>−1</sup> more stable than the folded conformer (Fig. 4). The five-membered thiophene rings in **ddTCO** may reduce the steric hindrance in the fjord region, resulting in a small torsion angle for the twisted conformer and thereby suppressing destabilization in the twisted conformer of **ddTCO**. Indeed, as shown in Fig. 4, the dihedral angle of the twisted conformer of bianthrone is 59.5°, much larger than that of **ddTCO** (52.3°). We also compared the energies of the corresponding singlet carbenes and dimers (Fig. S11, ESI†), and found a small difference in the formation energies of the folded conformers between bianthrone and **ddTCO**. However, the formation energy of the twisted conformers is more negative for **ddTCO** than for bianthrone. This suggests that the thermodynamic stability of the conformers of BAEs is more strongly influenced by the structure of the twisted

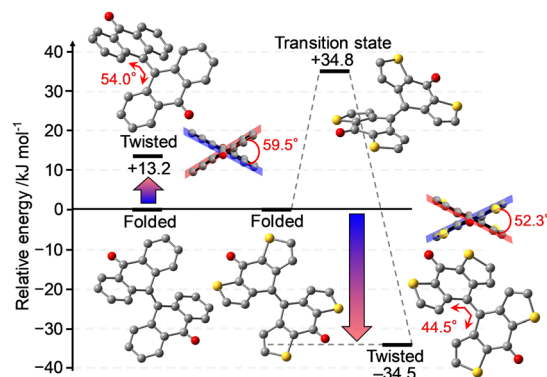


**Fig. 4** Gibbs free energy diagram of folded and twisted conformers of bianthrone and **ddTCO** in the closed-shell singlet state at the B3LYP-D3BJ/6-31G(d) level at 298 K. The Gibbs free energy of the folded conformer is set at zero. Hydrogen atoms are omitted for clarity.

conformer than by that of the folded conformer. The energy barrier between the twisted and folded conformers of **ddTCO** was calculated to be 69.3 kJ mol<sup>−1</sup> relative to the twisted conformer (Fig. 4), indicating that the two conformers are in thermal equilibrium at room temperature, like typical BAEs. However, because of the large energy difference between the twisted and folded conformers in **ddTCO**, the twisted conformer is predominant, as observed in the <sup>1</sup>H NMR and the UV-vis absorption spectra. The triplet state of **ddTCO** was calculated to be 25.6 kJ mol<sup>−1</sup> higher in energy than the singlet state twisted conformer at 298 K (Fig. S12, ESI†). In the ESR spectrum, the triplet signal was not observed (Fig. S13, ESI†), confirming that the ground state is singlet. From TD-DFT calculations, the S<sub>0</sub> → S<sub>1</sub> transition at 599 nm and the S<sub>0</sub> → S<sub>6</sub> transition at 420 nm were determined for the twisted conformer of **ddTCO** (Table S2, ESI†) and found to agree with the experimental absorption spectrum (Fig. S14, ESI†). In the folded conformer, the lowest energy-allowed transition was the S<sub>0</sub> → S<sub>2</sub> transition in the UV region at 438 nm (Table S3, ESI†).

Finally, the electrochemical and semiconductor properties of the thiophene-fused diphenylquinones were investigated. **ddTCO**, **ddTCO-Me**, and **ddTCO-Bu** showed irreversible oxidation and reversible reduction waves in the cyclic voltammograms (Fig. 5a and Fig. S15, ESI†). Interestingly, two reversible peaks were observed in the cathodic CV, which may correspond to the formation of radical anion and dianion species with aromatic resonance structures (Fig. 5a).<sup>15</sup> The first reduction potentials of **ddTCO**, **ddTCO-Me**, and **ddTCO-Bu** were −0.655, −0.680, and −0.698 V, respectively, from which the LUMO energy levels were calculated to be −4.15, −4.12, and −4.10 eV (Table 1). These LUMO energy levels are deeper than that of **ddTCB** (−3.99 eV)<sup>10a</sup> and comparable to those of typical n-type semiconductors.<sup>16</sup> Therefore, we fabricated organic field-effect transistors (OFETs) using these compounds and evaluated their semiconductor properties. To evaluate the charge transport properties, we fabricated OFETs with top-gate bottom-contact (TGBC) structures<sup>17</sup> using **ddTCO-Bu**, which has the highest solubility and good film-forming properties. Uniform thin films could not be obtained from **ddTCO** and **ddTCO-Me**, and they did





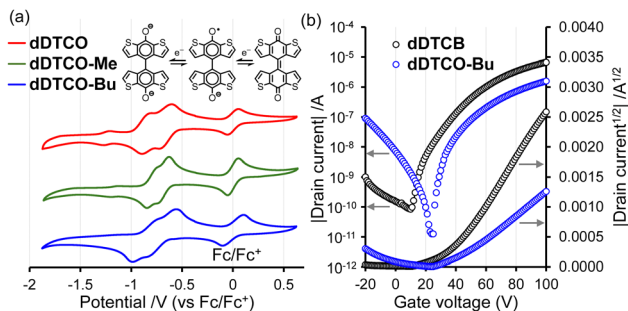


Fig. 5 (a) Cathodic cyclic voltammetry data of thiophene-fused diphenobenzoquinones in dichloromethane containing 0.1 M  $\text{Bu}_4\text{NPF}_6$  at the scan rate of  $100 \text{ mV s}^{-1}$ . (b) Transfer curves of **dDTCB** and **dDTCO-Bu** of OFETs.

not show FET characteristics. Owing to its deep LUMO energy level, **dDTCO-Bu** exhibited an n-type behavior with a moderate threshold voltage of 39.0 V and a high current on/off ratio of  $1.3 \times 10^5$  in n-channel operation (Fig. 5b), suggesting that the twisted diphenobenzoquinones are a promising building block for n-type semiconductor materials. The maximum electron mobility ( $\mu_e$ ) of **dDTCO-Bu** in five cells was  $5.0 \times 10^{-4} \text{ cm}^2 \text{ V}^{-1} \text{ s}^{-1}$ , which was lower than that of **dDTCB** (Table S4,  $2.0 \times 10^{-3} \text{ cm}^2 \text{ V}^{-1} \text{ s}^{-1}$ , ESI†). This may be due to the large steric hindrance of the four butyl groups with different tilt angles. Because **dDTCO** does not contain alkyl groups, it may exhibit superior n-type semiconductor properties. However, owing to its poor film-forming properties in wet processes, OFET evaluation was not possible. By forming films through vapor deposition, it may be possible to create superior OFET devices with **dDTCO**.

In summary, we performed an investigation of the photo-physical properties of diphenobenzoquinones fused with thiophene rings. By substituting thiophene rings for the benzene rings in bianthrone, the twisted conformer became more thermodynamically stable than the folded conformer, and the thiophene-fused BAEs were found to exist in the twisted conformer both in the solid state and in solution. The thiophene-fused diphenobenzoquinones possess deep LUMO energy levels, and thin films of **dDTCO-Bu** exhibit clear n-type semiconductor characteristics. The highly twisted BAE structure effectively reduces the HOMO–LUMO gap and is therefore a new molecular design for the development of conjugated molecules with strong absorption in the visible region or organic semiconductors.

This research was supported by JSPS (KAKENHI JP22K14666 and JP22K14745) and the Izumi Science and Technology Foundation. We thank Dr Kenji Komaguchi (Hiroshima University) for his kind support on ESR measurements.

## Data availability

The data supporting this article have been included as part of the ESI.† Crystallographic data for **dDTCO**, **dDTCO-Me**, and **dDTCO-Bu** has been deposited at the CCDC under 2363404–2363406.†

## Conflicts of interest

There are no conflicts to declare.

## Notes and references

- (a) L. Li, X. Dong, J. Li and J. Wei, *Dyes Pigm.*, 2020, **183**, 108756; (b) C. Yin, X. Li, Y. Wang, Y. Liang, S. Zhou, P. Zhao, C.-S. Lee, Q. Fan and W. Huang, *Adv. Funct. Mater.*, 2021, **31**, 2104650; (c) Y. Sun, P. Sun, Z. Li, L. Qu and W. Guo, *Chem. Soc. Rev.*, 2022, **51**, 7170; (d) Y. Ni and J. Wu, *Tetrahedron Lett.*, 2016, **57**, 5426.
- (a) C. Wenstrup, M. J. Regimbald-Kmel, D. Müller and P. Comba, *Angew. Chem., Int. Ed.*, 2016, **55**, 14600; (b) J. I. Wu, N. J. R. van Eikema Hommes, D. Lenoir and S. M. Bachrach, *J. Phys. Org. Chem.*, 2019, **32**, e3965; (c) Y. Hamamoto, Y. Hirao and T. Kubo, *J. Phys. Chem. Lett.*, 2021, **12**, 4729; (d) T. Nishiuchi, S. Aibara, H. Sato and T. Kubo, *J. Am. Chem. Soc.*, 2022, **144**, 7479; (e) B. Prajapati, M. D. Ambhore, D.-K. Dang, P. J. Chmielewski, T. Lis, C. J. Gómez-García, P. M. Zimmerman and M. Stepień, *Nat. Chem.*, 2023, **15**, 1541.
- (a) P. U. Biedermann, J. J. Stezowski and I. Agranat, *Eur. J. Org. Chem.*, 2001, 15234; (b) P. U. Biedermann, J. J. Stezowski and I. Agranat, *Chem. Commun.*, 2001, 954.
- A. Takai, D. J. Freas, T. Suzuki, M. Sugimoto, J. Labuta, R. Haruki, R. Kumai, S. Adachi, H. Sakai, T. Hasobe, Y. Matsushita and M. Takeuchi, *Org. Chem. Front.*, 2017, **4**, 650.
- S. Hashimoto, T. Ikuta, K. Shiren, S. Nakatsuka, J. Ni, M. Nakamura and T. Hatakeyama, *Chem. Mater.*, 2014, **26**, 6265.
- (a) W. T. Grubb and G. B. Kistiakowsky, *J. Am. Chem. Soc.*, 1950, **72**, 419; (b) Y. Tapuhi, O. Kalisky and I. Agranat, *J. Org. Chem.*, 1979, **44**, 1949.
- (a) S. Pogodin, M. R. Suissa, A. Levy, S. Cohen and I. Agranat, *Eur. J. Org. Chem.*, 2008, 2887; (b) O. Ivashenko, H. Logtenberg, J. Areephong, A. C. Coleman, P. V. Wesenhagen, E. M. Geertsema, N. Heureux, B. L. Feringa, P. Rudolf and W. R. Browne, *J. Phys. Chem. C*, 2011, **115**, 22965; (c) Y. Hirao, Y. Hamamoto, N. Nagamachi and T. Kubo, *Phys. Chem. Chem. Phys.*, 2019, **21**, 12209; (d) Y. Hirao, Y. Hamamoto and T. Kubo, *Chem. – Asian J.*, 2022, **17**, e202200121.
- (a) A. Levy, S. Cohen, S. Pogodin and I. Agranat, *Struct. Chem.*, 2015, **26**, 1565; (b) K. Rakstys, S. Paek, G. Grancini, P. Gao, V. Jankauskas, A. M. Asiri and M. K. Nazeeruddin, *ChemSusChem*, 2017, **10**, 3825; (c) Y. Hirao, N. Nagamachi, K. Hosoi and T. Kubo, *Chem. – Asian J.*, 2018, **13**, 510; (d) T. Suzuki, H. Okada, T. Nakagawa, K. Komatsu, C. Fujimoto, H. Kagi and Y. Matsuo, *Chem. Sci.*, 2018, **9**, 475; (e) Y. Wang, Y. Ma, K. Ogumi, B. Wang, T. Nakagawa, Y. Fu and Y. Matsuo, *Commun. Chem.*, 2020, **3**, 93; (f) K. Ogumi, K. Nagata, Y. Takimoto, K. Mishiba and Y. Matsuo, *J. Mater. Chem. C*, 2022, **10**, 11181; (g) K. Ogumi, K. Nagata, Y. Takimoto, K. Mishiba and Y. Matsuo, *Sci. Rep.*, 2022, **12**, 16997.
- (a) E. Molins, C. Miravittles, E. Espinosa and M. Ballester, *J. Org. Chem.*, 2002, **67**, 7175; (b) J. Luo, K.-W. Huang, H. Qu, X. Zhang, L. Zhu, H. S. O. Chan and C. Chi, *Org. Lett.*, 2010, **12**, 5660; (c) C.-Y. Chiu, H. Wang, F. G. Brunetti, F. Wudl and C. J. Hawker, *Angew. Chem., Int. Ed.*, 2014, **53**, 3996; (d) K. Rakstys, M. Saliba, P. Gao, P. Gratia, E. Kamarauskas, S. Paek, V. Jankauskas and M. K. Nazeeruddin, *Angew. Chem., Int. Ed.*, 2016, **55**, 7464; (e) J. Xu, A. Takai, A. Bannaron, T. Nakagawa, Y. Matsuo, M. Sugimoto, Y. Matsushita and M. Takeuchi, *Mater. Chem. Front.*, 2018, **2**, 780; (f) B. Xiao, Y. Yang, S. Chen, Y. Zou, X. Chen, K. Liu, N. Wang, Y. Qiao and X. Yin, *Chem. – Eur. J.*, 2023, **29**, e202301055.
- (a) Y. Adachi, T. Nomura, S. Tazuhara, H. Naito and J. Ohshita, *Chem. Commun.*, 2021, **57**, 1316; (b) K. Yamada, Y. Adachi and J. Ohshita, *Chem. – Eur. J.*, 2023, **29**, e202302370.
- (a) D. Mitsui, Y. Mazaki and G. Yamamoto, Proceedings of 18th Symposium on Fundamental Organic Chemistry, 2006, DOI: [10.1149/kisoyuki.18.0.28.0](https://doi.org/10.1149/kisoyuki.18.0.28.0); (b) D. Mitsui, Y. Mazaki and G. Yamamoto, Synthesis, Structures, and Properties of Thiophene Analogues of Bianthrone, at the ISNA-12, Hyogo, Japan, July 2007.
- (a) D. W. H. MacDowell and James C. Wisowaty, *J. Org. Chem.*, 1971, **36**, 4004; (b) D. W. H. MacDowell and F. L. Ballas, *J. Org. Chem.*, 1974, **39**, 2239.
- D. E. Nicodem and M. F. V. da Cunha, *J. Photochem. Photobiol., A*, 1997, **107**, 165.
- Y.-J. Cheng, S.-H. Yang and C.-S. Hsu, *Chem. Rev.*, 2009, **109**, 5868.
- S. Neron, M. Morency, L. Chen, T. Maris, D. Rochefort, R. Iftimie and J. D. Wuest, *J. Org. Chem.*, 2022, **87**, 7673.
- H. Sun, X. Guo and A. Facchetti, *Chemistry*, 2020, **6**, 1310.
- T. Mikie, K. Okamoto, Y. Iwasaki, T. Koganezawa, M. Sumiya, T. Okamoto and I. Osaka, *Chem. Mater.*, 2022, **34**, 2717.

